INFLUENCE OF TITANIUM ADDITIONS ON THE ELECTROCHEMICAL BEHAVIOUR OF NiCr/Ti LASER CLADDED COATINGS

D. N. Avram[1], C. M. Davidescu[2], M. L. Dan[1], E. M. Stanciu[3], A. Pascu[3], J. C. Mirza-Rosca[4]*, H. Iosif[4]

[1] Faculty of Industrial Chemistry and Environmental Engineering, Politehnica University Timisoara, 2 Piata Victoriei, Timisoara, Romania
[2]Renewable Energy Research Institute-ICER, Politehnica University Timisoara, 138 Gavril Musicescu Street, Timisoara Romania
[3]Materials Engineering and Welding Depart., Transilvania University of Brasov, 29 Eroilor Blvd., 500036, Brasov, Romania
[4]Depart. of Mechanical Engineering, Las Palmas de Gran Canaria University, Tafira, Spain
*Corresponding author's e-mail address: julia.mirza@ulpgc.es

ABSTRACT

In this research, the electrochemical evaluation of NiCr/Ti laser cladded coatings in simulated polymer electrolyte membrane fuel cells (PEMFCs) environment was investigated. The Laser Cladding technique was used to develop protective coatings on mild steel substrate using NiCr-based powders mixed with 12.5, 15, 17.5 and 20 wt.% Ti additions. The samples were tested at room temperature in Na_2SO_4 0.1M + 0.1 ppm F-. The potentiodynamic polarization curves are presented before and after the samples were subjected to accelerated stress tests, for 6 hours each, at +0.736 V (cathodic environment) and at -0.493 V (anodic environment). Afterwards, scanning electron microscopy (SEM) was used to investigate the effect of Ti addition in terms of morphology. Energy-dispersive X-ray spectroscopy (EDS) was performed for chemical evaluation of the surface after corrosion tests.

KEYWORDS: laser cladding, corrosion, advanced materials, titanium, NiCr/Ti.

1. INTRODUCTION

Human activity has dramatically changed the surrounding environment, with greenhouse gas emissions (especially CO_2 and CH_4) being the main reason for global warming. Overwhelmingly, it is forecasted that fossil fuels will increase up to 25% of the energy used worldwide by 2040. Shaping a sustainable future and replacing conventional energy production with eco-friendly alternatives has become nowadays a priority [1]. Among alternative energy production such as wind, sunlight, geothermal heat or biomass, fuel cells can become a reliable solution to the worldwide demand for energy. It has the advantage of converting the chemical energy of hydrogen and oxygen to electrical energy, on condition that the fuels are continuously supplied within the fuel cell. These electrochemical devices can provide an important contribution to reducing the dependence on fossil fuels, as they can be used in transport applications and stationary or portable power systems [2], [3].

PEMFCs have a clean method of energy production, are quiet in operating, have fast response, high power densities and are recognized for their promising transport applications [4]. One of the most important components of PEMFCs is the bipolar plate (BP). So far, there has been a lot of research on different types of suitable materials, such as graphite-based, metallic-based and polymeric composite-based.

The interest in carbon-based BPs has shifted to metallic-based BPs over the years [5], [6]. In order to overcome surface corrosion and reduce the contact resistance on the metallic plates, various types of protective coatings were investigated [7]. Chemical vapor deposition [8], electrophoretic deposition [9], arc ion plating [10], or even high-velocity oxygen fuel [11] have been some of the techniques used in literature to apply a protective coating.

In our latest investigations, we have presented that laser cladding technology might be used as a manufacturing option to produce protective coatings on mild steel substrate with potential application for metallic bipolar plates [12], [13].

The main objective of this research was to investigate the influence of Ti additions ranging from 12.5 to 20 wt.% on the corrosion properties of

© *Galati University Press, 2022*

Date of submission/acceptance: 06.11.2022/15.12.2022
https://doi.org/10.35219/awet.2022.10

NiCr/Ti protective coatings. Four samples obtained by laser cladding of NiCr/Ti (NiCr + 12.5%, 15%, 17.5% and 20%Ti) on mild steel substrate were investigated. The impact of titanium addition was studied using potentiodynamic polarization curves, before and after the samples were subjected to cathodic/anodic accelerated stress tests, for 6 hours each.

Afterwards, the morphology and microstructure of the cladded samples were investigated using scanning electron microscopy.

2. MATERIALS AND METHODS

2.1 Materials

NiCr-based powder (MetcoClad 625F, Oerlikon Metco, Switzerland) with different wt.% titanium powder, 99% pure (Metco 4010A, Oerlikon Metco, Switzerland), was deposited onto previously polished mild steel substrates with dimensions of 60 x 25 x 5 mm. The chemical compositions of the mild steel (see Table 1) and NiCr-based powder are presented (see Table 2). The feedstock material MetcoClad 625F was reinforced by additions of 12.5, 15, 17.5 and 20 wt.% Ti and mechanically mixed to obtain a homogenous powder.

Table 1. Chemical composition of 1010 mild steel substrate, according to the manufacturer [14]

Fe [%]	C [%]	Mn [%]	Si [%]	P [%]	Ni [%]	Cr [%]	Ti [%]	V [%]
Bal.	0.08 - 0.13	0.03-0.06	0.02	0.03	0.08	0.02	0.08	0.08

A Coherent F1000 diode laser with a wavelength of 975 nm was employed to manufacture the coatings. The laser was mounted on a Cloos six-axis robotic arm and MetcoClad 625F was fed into a processing head type Precitec WC 50. The powder was transported to the cladding head by a feeding system type Termach AT-1200 HPHV. Argon was used as shielding and carrier gas. The parameters used to deposit the MetcoClad 625F clads on the mild steel substrate were previously optimised [15]: powder preheating = 70°C; laser power = 859 W; scanning speed = 40 cm/min; carrier gas flow = 15.1 L/min; focal distance = 200 mm; overlap between subsequent tracks = 45%.

Table 2. Chemical composition of MetcoClad 625F, according to the manufacturer [16]

Ni [%]	Cr [%]	Mo [%]	Nb [%]	Fe [%]	Other [%]
Bal.	20.0 - 23.0	8.0-10.0	3.0-5.0	<5.0	<2.0

2.2 Equipment

A potentiostat/galvanostat model SP 150 (Bio Logic Science Instruments, France) was used for the electrochemical evaluation of NiCr/Ti cladded samples. The electrochemical cell used was a three-electrode system, with platinum gauze as the counter-electrode and the Ag/AgCl as the reference electrode. Before conducting the investigations, the cladded samples were ground with different abrasive papers and polished until the surface had a mirror-like reflection. The electrolyte used in the experimental part consisted of a solution of Na_2SO_4 0.1M (acidulated with H_2SO_4 at pH = 5) + 0.1 ppm F-. The potentiodynamic polarization technique was employed in the potential range ± 250 mV vs. OCP, using a 1 mV/s scan rate.

The potentiodynamic polarization curves are presented before and after the samples were subjected to an accelerated stress test, for 6 hours each, at +0.736 V (cathodic environment) and at -0.493 V (anodic environment). Afterwards, scanning electron microscopy (SEM - Quanta FEG 250, FEI, USA) using a backscattered electron detector (BSD) was employed to investigate the influence of titanium additions in terms of morphology. Energy-dispersive X-ray spectroscopy (EDS) was performed for chemical evaluation of the surface after corrosion tests.

3. RESULTS AND DISCUSSION

The potentiodynamic polarization curves of the coated samples tested in Na_2SO_4 0.1M + 0.1 ppm F- at room temperature are presented in figure 1. The Tafel plots have been recorded at a scan rate of 1mV/s, before conducting the accelerated stress test.

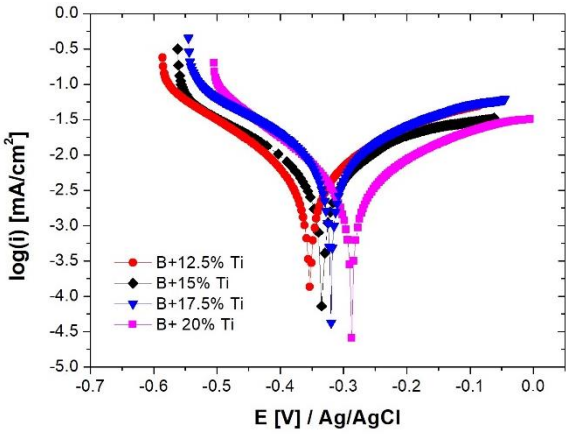

Fig. 1. Potentiodynamic polarization curves of coated samples tested in Na_2SO_4 0.1M + 0.1 ppm F- at room temperature recorded at 1mV/s scan rate.

In table 3 are presented the polarization parameter values using the Tafel extrapolation method from EC-lab software. From the presented

values, it can be observed that the increase of titanium additions within the coatings increases the polarization resistance (RP) and decreases the corrosion rates (CR). The cladded sample with 20% Ti addition has the lowest corrosion current density (i_{corr}) and corrosion rate and the highest polarization resistance of the tested samples.

Table 3. Polarization parameters for samples tested in Na_2SO_4 0.1M + 0.1 ppm F- at room temperature recorded at 1mV/s scan rate

Samples	i_{corr} [µA cm^{-2}]	E_{corr} [mV]	-b_c [mV dec^{-1}]	b_a [mV dec^{-1}]	R_p [kΩ cm^2]	C_R [mm/yr]
B+12.5%Ti	1.119	-353	170	147	30	0.0099
B+15%Ti	1.026	-334	165	141	32	0.0087
B+17.5%Ti	1.010	-319	160	138	32	0.0085
B+20%Ti	0.942	-304	194	144	38	0.0078

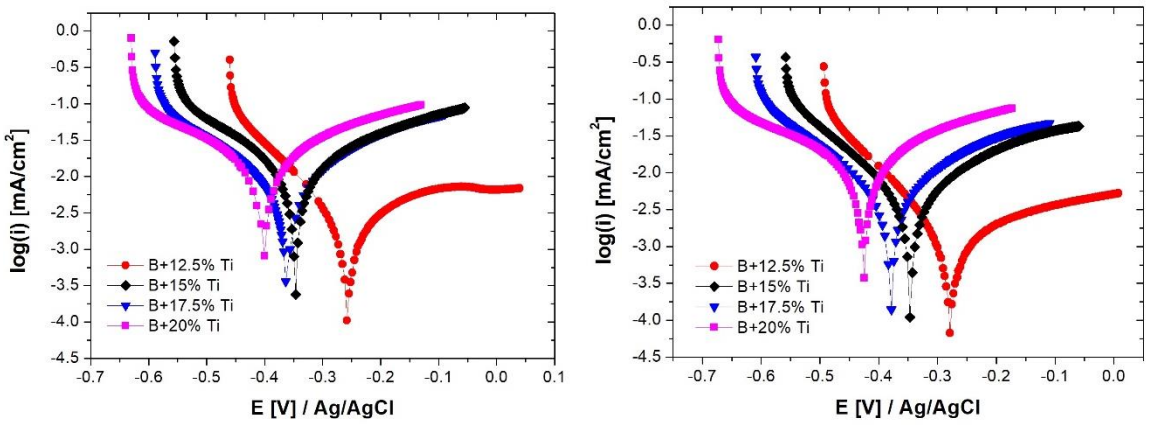

Fig. 2. Potentiodynamic polarization curves of samples in Na_2SO_4 0.1M + 0.1 ppm F-, after accelerated stress test for 6h in: a) cathodic environment at +0.736 V; b) anodic environment at -0.493 V

Table 4. Polarization parameters of samples in Na_2SO_4 0.1M + 0.1 ppm F^- after accelerated stress test for 6h in cathodic environment at +0.736 V and anodic environment at -0.493 V

Samples	i_{corr} [µA cm^{-2}]	E_{corr} [mV]	-b_c [mV dec^{-1}]	b_a [mV dec^{-1}]	R_p [kΩ cm^2]	C_R [mm/yr]
Cathodic environment +0.736 V						
B+12.5%Ti	0.468	-258	184	127	70	0.0041
B+15%Ti	1.540	-346	162	129	20	0.0138
B+17.5%Ti	1.782	-363	176	145	19	0.0152
B+20%Ti	3.020	-399	181	151	12	0.0251
Anodic environment -0.493 V						
B+12.5%Ti	0.446	-279	247	139	87	0.0039
B+15%Ti	1.211	-346	198	145	30	0.0104
B+17.5%Ti	1.488	-379	203	158	26	0.0126
B+20%Ti	3.449	-424	221	164	12	0.0287

The polarization resistance (R_p) was calculated from the Stern-Geary equation, where b_a and b_c are the anodic and cathodic Tafel slopes (V) and i_{corr} is the corrosion current density (A·cm^{-2}), as presented in the equation bellow:

$$R_p = \frac{b_a \cdot b_c}{i_{corr} \cdot 2.303(b_a + b_c)} \quad (1)$$

The corrosion rate (C_R) of the laser-coated samples was determined using the ASTM G 102-98 standard [17], where K_1 is a constant equal to 0.00327 (mm·g·µA^{-1}·cm^{-1}·yr^{-1}), i_{corr} is the corrosion current density (µA cm^{-2}), ρ is the density (g·cm^{-3}) and EW is the equivalent weight (dimensionless).

$$C_R = K_1 \frac{i_{corr}}{\rho} EW \quad (2)$$

In figure 2 are presented the potentiodynamic polarization curves of the coated samples recorded at a scan rate of 1mV/s, after the accelerated stress test. The Tafel plots of samples after the accelerated stress test for 6h in a cathodic environment at +0.736 V are presented in figure 2a and in an anodic environment at -0.493 V in figure 2b.

Table 4 summarizes the values of polarization parameters using the Tafel extrapolation method from EC-lab software of the samples after the accelerated stress test for 6h in the cathodic environment at +0.736 V and in the anodic environment at -0.493 V. It can be seen, that in both experiments, the increase of titanium additions within the coatings decreases the polarization resistance (RP) and increases the corrosion rates (CR).

The laser-cladded sample with 12.5% Ti addition showed the best results in terms of corrosion resistance. On the other hand, for laser-cladded samples with 15% or more Ti addition, the results worsened after the accelerated stress tests, in both cases.

After accelerated stress tests, in both cathodic and anodic environments, the NiCr laser-cladded sample with 20% Ti addition has the highest corrosion current density, highest corrosion rate and the lowest polarization resistance from the tested samples.

Fig. 3. SEM images of NiCr/Ti coatings with 15% Ti addition: a) 20% Ti addition at higher magnification; b) EDS spectrum of marked areas; c) 20% Ti addition at lower magnification; d) after accelerated stress

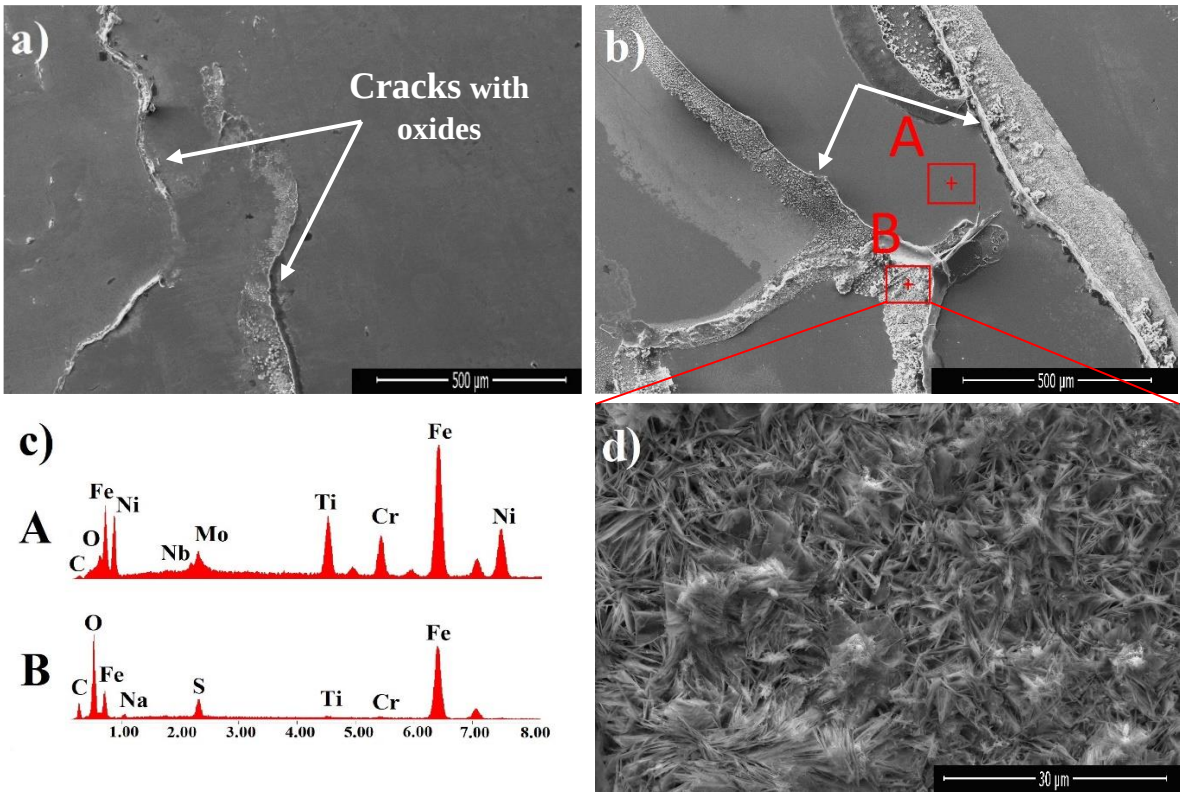

In figure 3 are presented SEM images of NiCr-based coatings with 15% Ti addition (figure 3a) and 20% Ti addition (figure 3b) after the samples were exposed to the accelerated stress test. It can be noticed that both samples present cracks and one can observe that the cracking susceptibility increases with Ti additions. This was observed after the corrosion test on the polished surface of the samples after the electrolyte infiltrated the coatings through the cracks.

The cracks appeared within the coatings due to large thermal phase transformation stress [18], which might be caused by the excess of Ti addition in the coating. These cracks allow the electrolyte to reach the substrate and promote oxidation as one can see from the EDS results presented in figure 3c. Compared to the coatings, the oxides present an acicular morphology (see figure 3d) and are rich in oxygen and iron. It can be observed as well that the rough surface of the oxide entraps Na and S, constituents of the electrolyte. The results are in accordance with the potentiodynamic polarization curves and polarization parameters presented previously.

4. CONCLUSIONS

New NiCr-based coatings with Ti additions ranging from 12.5% to 20% were deposited on low-carbon steel using laser cladding. The potentiodynamic polarization technique was used to study the corrosion

proprieties of the tested samples in Na_2SO_4 0.1M + 0.1 ppm F-, before and after submitting them under an accelerated stress test in cathodic (+0.736 V) and anodic environment (-0.493 V).

SEM and EDS analysis was employed to investigate the effect of Ti addition in terms of morphology and for chemical evaluation of the surface after corrosion tests.

From the experimental investigation, the following conclusions were taken:

- according to the potentiodynamic polarization curves, before conducting the accelerated stress test, the increase of titanium additions within the coatings decreased the corrosion rates, and the best results were obtained for the laser-cladded sample with 20 wt.% Ti addition;
- after accelerated cathodic/anodic stress tests, the increase of titanium additions within the coatings increased the corrosion rates and among the four samples tested, the best result was obtained for the laser-cladded sample with 12.5 wt.% Ti addition;
- additions from 15 to 20 wt.% Ti increased the cracking susceptibility and reduced the coating performances in terms of corrosion resistance.

REFERENCES

[1]. **Crosthwaite J.**: *Just transition to a sustainable future without 'fossil'gas*, Academic rigour, 2020, p. 240.

[2]. **Hoogers G.**, *Fuel cell technology handbook*, CRC press, 2002.

[3]. **Martinez J. G.**, *Nanotechnology for the energy challenge 2nd Edition*, Wiley-VCH, 2013.

[4]. **Chen X., Long S., He L., Wang C., Chai F., Kong X., Tu Z.**, *Performance evaluation on thermodynamics-economy-environment of PEMFC vehicle power system under dynamic condition*, Energy Conversion and Management, vol. 269, 2022, 116082.

[5]. **Wang H., Turner J. A.**, *Reviewing metallic PEMFC bipolar plates*, Fuel cells, vol. 10, no. 4, 2010, pp. 510-519.

[6]. **Branco C. M., El-kharouf A., Du S.**, *Materials for Polymer Electrolyte Membrane Fuel Cells (PEMFCs): Electrolyte Membrane, Gas Diffusion Layers, and Bipolar Plates*, Reference Module in Materials Science and Materials Engineering, Elsevier, 2017, pp. 1-11.

[7]. **Wind J., Späh R., Kaiser W., Böhm G.**, *Metallic bipolar plates for PEM fuel cells*, Journal of Power Sources, vol. 105, 2002, pp. 256-260.

[8]. **Fukutsuka T., Yamaguchi T., Miyano S. I., Matsuo Y, Sugie Y., and Ogumi Z.**, *Carbon-coated stainless steel as PEFC bipolar plate material*, Journal of Power Sources, vol. 174, no. 1, 2007, pp. 199-205.

[9]. **Myung S.T., Kumagai M., Asaishi R., Sun Y. K., Yashiro H.**, *Nanoparticle TiN-coated type 310S stainless steel as bipolar plates for polymer electrolyte membrane fuel cell*, Electrochemistry Communications, vol. 10, no. 3, 2008, pp. 480-484.

[10]. **Zhang D., Duan L., Guo L., Wang Z., Zhao J., Tuan W. H., Niihara K.**, *TiN-coated titanium as the bipolar plate for PEMFC by multi-arc ion plating*, International journal of hydrogen energy, Vol. 36, no. 15, 2011, pp. 9155-9161.

[11]. **Hung Y., Tawfik H., and Mahajan D.**, *Durability and characterization studies of chromium carbide coated aluminum fuel cell stack*, International Journal of Hydrogen Energy, vol. 41, no. 28, 2016, pp. 12273-12284.

[12]. **Avram D. N., Davidescu C. M., Dan M. L., Mirza-Rosca J. C., Hulka I., Pascu A., Stanciu E. M.**, *Electrochemical Evaluation of Protective Coatings with Ti Additions on Mild Steel Substrate with Potential Application for PEM Fuel Cells*, Materials, vol. 15, 2022, 5364

[13]. **Avram D. N., Davidescu C. M., Dan M. L., Mirza-Rosca J. C., Hulka I., Stanciu E. M., Pascu A.**, *Corrosion resistance of NiCr (Ti) coatings for metallic bipolar plates*, Materials Today: Proceedings, 2022, In press, doi: https://doi.org/10.1016/j.matpr.2022.09.007

[14]. *** https://matmatch.com/materials/minfc37596-sae-j403-grade-1010, accesed on 18.10.2022.

[15]. **Hulka I., Utu I. D., Avram D. N., Dan M. L., Pascu A., Stanciu E. M., Roata I. C.**, *Influence of the Laser Cladding Parameters on the Morphology,Wear and Corrosion Resistance of WC-Co/NiCrBSi Composite Coatings*, Materials, vol. 14, 2021, 5583.

[16]. *** https://www.oerlikon.com/am/en/about-us/media/oerlikon-metco-offers-materials-newly-optimized-for-additive-manufacturing-applications/, Material Product Data Sheet Nickel-Based Superalloy Powders for Laser Cladding and Laser-Additive Manufacturing.

[17]. *** Standard Practice for Calculation of Corrosion Rates and Related Information from Electrochemical Measurements, ASTM G 102-98, (Reapproved 1999).

[18]. **Yanan L., Ronglu S., Wei N., Tiangang Z., Yiwen L.**, *Effects of CeO2 on microstructure and properties of TiC/Ti2Ni reinforced Ti-based laser cladding composite coatings*, Optics and Lasers in Engineering, vol. 120, 2019, pp. 84-94.

.